

# UC San Diego

## UC San Diego Previously Published Works

### Title

An ice core record of near-synchronous global climate changes at the Bølling transition

### Permalink

<https://escholarship.org/uc/item/6690w1nb>

### Journal

Nature Geoscience, 7(6)

### ISSN

1752-0894

### Authors

Rosen, Julia L  
Brook, Edward J  
Severinghaus, Jeffrey P  
et al.

### Publication Date

2014-06-01

### DOI

10.1038/ngeo2147

Peer reviewed

# An ice core record of near-synchronous global climate changes at the Bølling transition

Julia L. Rosen<sup>1</sup>, Edward J. Brook<sup>1\*</sup>, Jeffrey P. Severinghaus<sup>2</sup>, Thomas Blunier<sup>3</sup>, Logan E. Mitchell<sup>1</sup>, James E. Lee<sup>1</sup>, Jon S. Edwards<sup>1</sup> and Vasileios Gkinis<sup>3</sup>

**The abrupt warming that initiated the Bølling–Allerød interstadial was the penultimate warming in a series of climate variations known as Dansgaard–Oeschger events. Despite the clear expression of this transition in numerous palaeoclimate records, the relative timing of climate shifts in different regions of the world and their causes are subject to debate. Here we explore the phasing of global climate change at the onset of the Bølling–Allerød using air preserved in bubbles in the North Greenland Eemian ice core. Specifically, we measured methane concentrations, which act as a proxy for low-latitude climate, and the  $^{15}\text{N}/^{14}\text{N}$  ratio of  $\text{N}_2$ , which reflects Greenland surface temperature, over the same interval of time. We use an atmospheric box model and a firn air model to account for potential uncertainties in the data, and find that changes in Greenland temperature and atmospheric methane emissions at the Bølling onset occurred essentially synchronously, with temperature leading by  $4.5^{+21}_{-24}$  years. We cannot exclude the possibility that tropical climate could lag changing methane concentrations by up to several decades, if the initial methane rise came from boreal sources alone. However, because even boreal methane-producing regions lie far from Greenland, we conclude that the mechanism that drove abrupt change at this time must be capable of rapidly transmitting climate changes across the globe.**

Like other Dansgaard–Oeschger (D–O) events of the last glacial period, the Bølling transition is marked by an abrupt Northern Hemisphere warming<sup>1</sup>, pronounced changes in tropical climate<sup>2</sup> and an increase in atmospheric methane<sup>3</sup>. The prevailing explanation for D–O warmings invokes perturbations to the freshwater budget of the North Atlantic that trigger changes in the strength of the meridional overturning circulation<sup>4</sup> (MOC). This switch then initiates climate changes in distant regions through global teleconnections that, among other things, displace the mean position of the intertropical convergence zone<sup>5</sup> (ITCZ) and alter tropical rainfall patterns<sup>2,6</sup>. However, despite some empirical evidence for changes in ocean circulation across the Bølling transition<sup>7,8</sup>, this explanation is not universally accepted. This is partially due to the fact that model results vary significantly in the amount of freshwater forcing required, the amplitude of results, and their timing<sup>9,10</sup>, particularly when simulating a resumption of circulation, raising the possibility that other mechanisms may be at play.

In principle, differentiating between potential drivers of abrupt climate changes can be accomplished by precisely determining the phasing of climate responses in geographically distant regions under the assumption that the triggering region will change first. Methane and the  $\delta^{15}\text{N}$  of  $\text{N}_2$  in Greenland ice cores both registered abrupt climate changes during the last glacial period, but each represents regionally distinct processes, enabling such phase relationships to be analysed<sup>11,12</sup>. When measured in the same core, the fact that these gases occur in the same trapped air allows leads and lags to be stratigraphically constrained regardless of age scale uncertainties.

Methane is an important greenhouse gas with globally distributed sources whose concentration changed in concert with Greenland temperature during the last glacial period<sup>3,13</sup>.

Today, the largest methane source region lies in the tropics<sup>14</sup>, with important source areas under the influence of the Asian monsoon, whose intensity varied in step with D–O events owing to poorly understood climatic teleconnections<sup>15</sup>. The tropics probably dominated methane variability to an even greater degree when the presence of large Northern Hemisphere ice sheets and pervasive permafrost inhibited boreal methane production<sup>3,16,17</sup>. This assumption is bolstered by new calculations of the inter-polar methane gradient<sup>18</sup>—a measure of the latitudinal distribution of sources—which confirm that changes in the tropical source can explain most of the methane concentration increase across the Bølling transition, validating its use as a proxy for tropical climate change at this time. However, ref. 18 also demonstrates that boreal sources contributed a non-negligible amount of methane to the Bølling increase, and we discuss the implications of this observation below.

The  $\delta^{15}\text{N}$  of atmospheric  $\text{N}_2$  provides a gas phase palaeothermometer for abrupt changes in surface temperature at an ice core site<sup>11,12</sup>. Gases become trapped in bubbles at a depth of 60–100 m in an ice sheet, at the bottom of the layer of densifying snow known as the firn, where the compaction of snow seals off pores from further gas exchange. As air mixes diffusively within the interconnected open pores of the firn, the isotopes of  $\text{N}_2$  fractionate gravitationally, leading to an enrichment of  $\delta^{15}\text{N}$ – $\text{N}_2$  at the bottom of the firn.  $\delta^{15}\text{N}$  also fractionates under the presence of a thermal gradient. Such a gradient persists following an abrupt climate change for several centuries until the ice at the close-off depth adjusts to the new surface temperature. This causes the heavy isotope to migrate towards the coldest region of the firn (the base, in the case of a warming), leading to a positive isotopic excursion in the ice core record that serves as a gas phase marker of local temperature change.

<sup>1</sup>College of Earth, Ocean, and Atmospheric Science, Oregon State University, Corvallis, Oregon 97331, USA, <sup>2</sup>Scripps Institution for Oceanography, University of California–San Diego, San Diego, California 92093, USA, <sup>3</sup>The Centre for Ice and Climate, Niels Bohr Institute, University of Copenhagen, DK-2100 Copenhagen, Denmark. \*e-mail: brooke@geo.oregonstate.edu

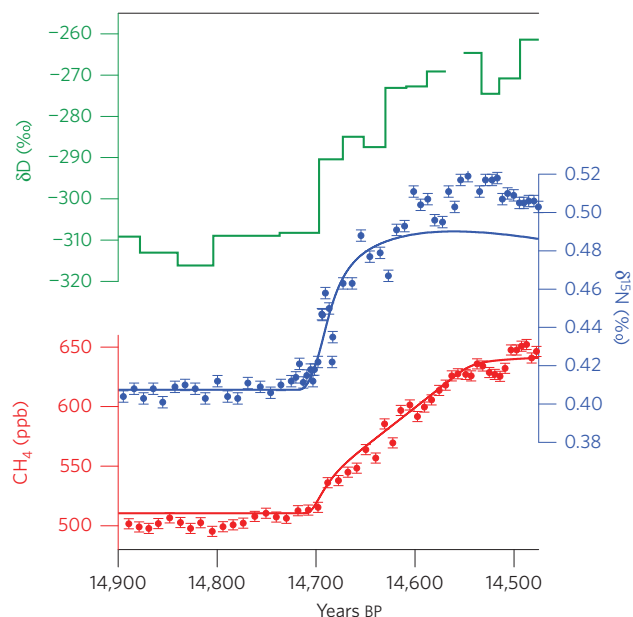


**Figure 1 |  $\delta D$ ,  $\delta^{15}N$  and methane data from the NEEM ice core at the Bølling transition.**  $\delta D$  values (green) are 55-cm averages plotted on the GICC05 ice age scale, converted to years BP (0 = AD 1950).  $\delta^{15}N$  (blue circles) and  $CH_4$  (red circles) are shown with their  $1\sigma$  standard deviations. All gas data are plotted on the chronology of ref. 36, converted to years BP (0 = AD 1950). Sample model results (solid blue and red lines) are also shown to illustrate the ability of the model to reproduce the gas record (Supplementary Text 1).

We measured  $CH_4$  and  $\delta^{15}N-N_2$  in the North Greenland Eemian (NEEM) ice core at high resolution across the Bølling transition (Fig. 1; Methods). Our data show that both gases respond to this climate change, and change synchronously in the ice core record (black vertical line in Fig. 2). The initial increase in both gases starts at 14,698 years BP (defined as 0 = AD 1950) with a relative uncertainty of 5 years due to the spacing of sample measurements. The increases are easily identifiable because the first data point of each transition far exceeds the envelope of previous variability, and the magnitude of the increase exceeds the analytical uncertainty of the measurement by a factor of 5 for  $CH_4$  and 8 for  $\delta^{15}N$ .

However, because we are actually interested in the timing of climate-driven changes in methane emissions, at least two additional processes must be considered. First, atmospheric mixing and the long tropospheric lifetime of methane smoothes the impact of an abrupt increase in methane emissions on the mixing ratio in air over Greenland<sup>19</sup>. Second,  $CH_4$  moves through the firn more quickly than  $N_2$  because of its greater diffusivity<sup>20</sup>. Thus, we simulate the evolution of both gases including these processes using a simple one-box atmospheric mixing model<sup>19</sup> and the Oregon State University firn air model<sup>21</sup> (Supplementary Text 1).

To account for the uncertainty in the measured NEEM data, we generate a cloud of 10,000 data realizations by adding normally distributed analytical error to each data point. We then fit a spline curve through each realization of the data. This step is justified because high-frequency variations, such as the  $\delta^{15}N-N_2$  reversal centred at 14,684 years BP (Fig. 2, grey shaded bar), are most likely due to irregularities in the physical properties of the firn and bubble closure processes, not to real changes in surface conditions (Supplementary Text 2). Such rapid changes in atmospheric values are unlikely, and in any case, cannot be rapidly communicated to the lock-in depth because of firn smoothing (for example, ref. 22). As firn heterogeneity cannot create or remove gas—it can only shift the depth at which changes are recorded—smoothing provides a good

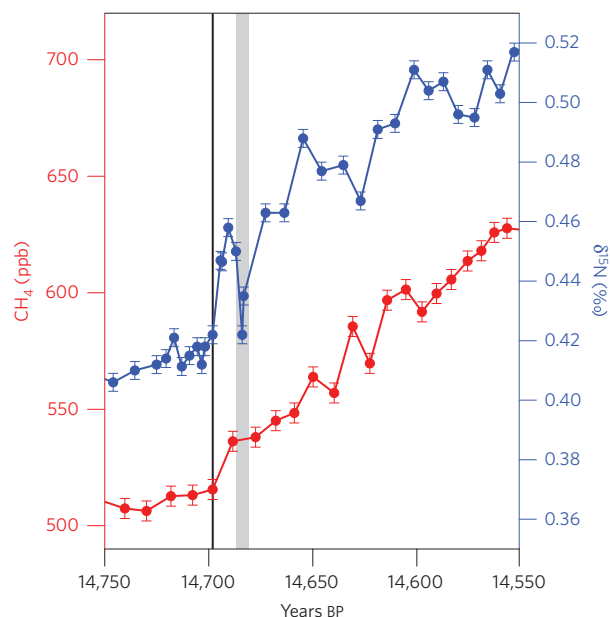


**Figure 2 | Detailed view of  $CH_4$  and  $\delta^{15}N$  from the NEEM ice core across the Bølling-Allerød transition.** Error bars represent the  $1\sigma$  standard deviations of  $\delta^{15}N$  (blue) and  $CH_4$  (red) measurements. The black vertical line marks the synchronous increase in both gases associated with the abrupt climate change. The grey shaded bar highlights the isotopic reversal in  $\delta^{15}N$  probably associated with firn heterogeneity and irregular bubble close-off (Supplementary Text 2).

approximation of gas behaviour in the firn given uniform bubble close-off, as assumed in the model.

To force the model, we use a total increase of  $6.5^\circ C$  from the mean pre-transition temperature because it produces the best fit to our data (Fig. 3a). However, without paired  $\delta^{40}Ar$  measurements to constrain changes in the gravitational component<sup>11</sup>, we cannot determine the true change in surface air temperature (the value used here is slightly lower than earlier estimates of the Bølling warming in Greenland using  $\delta^{15}N$  palaeothermometry from the GISP2 core<sup>11,23</sup>, but is consistent with new work suggesting that temperature changes at NEEM may have been smaller than at Summit<sup>24</sup>).

We explore 25 possible surface temperature functions starting with an instantaneous step function and increasing in duration by 2-yr increments to a 50-year linear increase (the slowest rate of change compatible with the water isotope record). As the shape of the forcing function may influence the inferred phase relationship, we use these scenarios to represent the full range of realistic possibilities while also producing reasonable fits to the smoothed NEEM data (Fig. 3b).

For methane, we generate a total source history in teragrams of  $CH_4$  per year that is then fed to a simple one-box atmospheric model<sup>19</sup>, assuming a lifetime of 8 years (Fig. 3c). We force the firn air model with the resulting atmospheric history. As the methane solution is also non-unique, we explore 30 possible source histories, generated systematically (Supplementary Text 3), that cover the likely range of emission scenarios and produce comparable model–data fits (Fig. 3d).

For each temperature or methane source history, we shift the resulting model ice core history generated by the firn model back and forth in time with respect to every 1 of the 10,000  $\delta^{15}N$  or  $CH_4$  data realizations until the best model–data correlation (R-values) is found for each realization (Fig. 3b,d). The shift in the model chronology (relative to 0 BP) associated with the best R-value provides the most likely time at which surface conditions began to change, a parameter we define as the start time. In total,

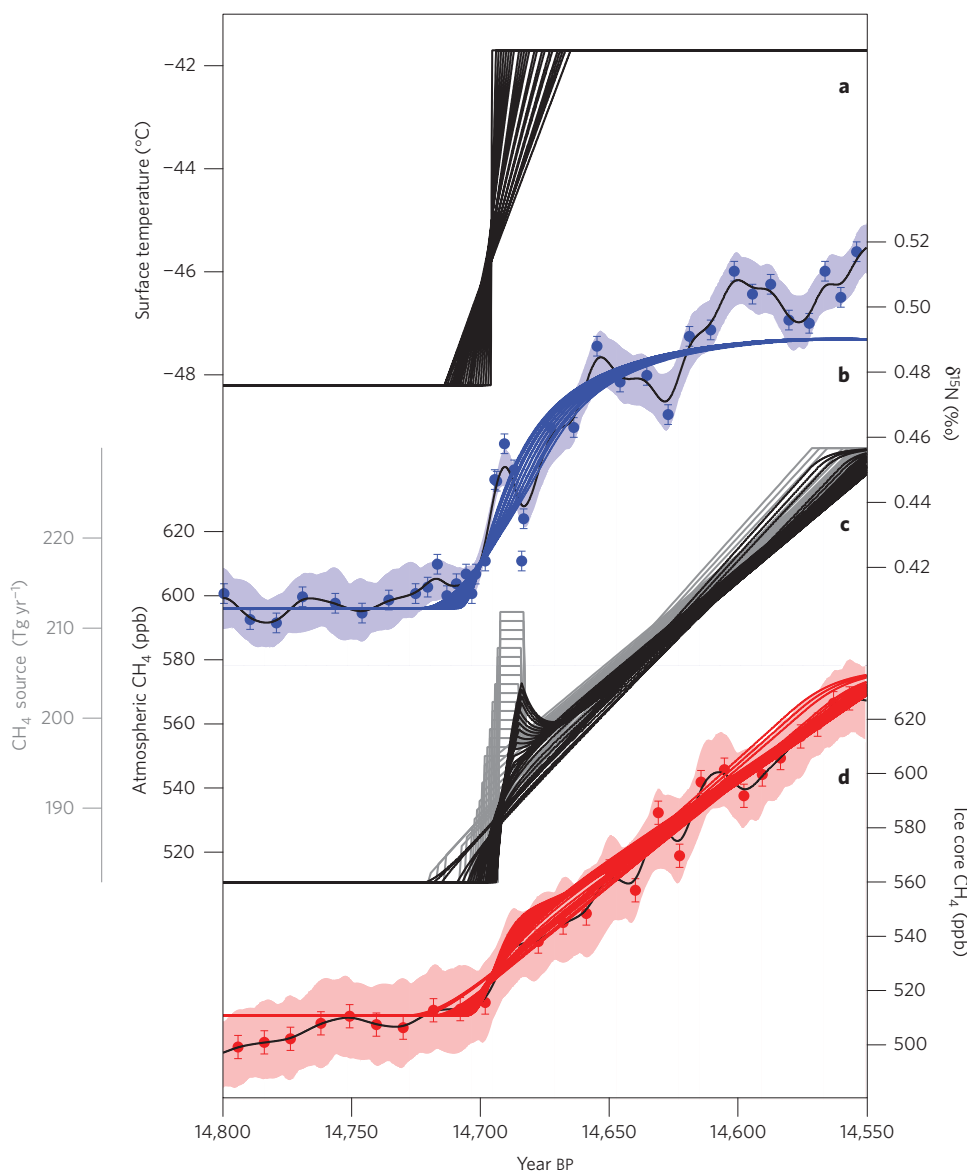


**Figure 3 | Model–data comparisons for a suite of possible surface scenarios.** **a**, Twenty-five temperature scenarios were used in the analysis (black lines; Supplementary Text 5). **b**, The measured NEEM  $\delta^{15}\text{N}$  data (blue circles) are shown with their  $1\sigma$  standard deviation along with the envelope of the Monte Carlo family of data realizations (blue shading), the average spline fit to the data (black solid line), and 25 firm model results (blue solid lines). **c**, Thirty methane source histories were used (grey lines) to produce associated atmospheric scenarios (black lines). **d**, The same as in **b**, but for methane.

we generate 25 sets (10,000 members each) of start times for the change in surface temperature and 30 sets for the change in methane emissions, one for each realization of each atmospheric scenario (Supplementary Text 4).

In a few cases, this procedure results in assigning identical start times to multiple scenarios (Supplementary Figs 4 and 5). We retain all scenarios here as we consider each to be equally likely, and note that using only scenarios with unique start times results in an even smaller phase lag between methane emissions and Greenland temperature (Fig. 3 and Supplementary Text 5). For every possible pair of atmospheric scenarios, we then calculate the time lag between the change in surface temperature over Greenland and the change in methane emissions by simply subtracting the methane start time from the temperature start time. We do this by pairing the start times for each of the 10,000  $\delta^{15}\text{N}$  and  $\text{CH}_4$  realizations in random order to avoid repeatedly pairing realizations that lead to a systematically biased phase lag. Last, we combine the resulting 7,500,000 estimates of methane leads into a single pooled histogram (Fig. 4).

The results show that methane emissions and Greenland temperature changed essentially synchronously with temperature leading by  $4.5^{+21}_{-24}$  years (95% confidence error bounds). Although this phase relationship may mirror the phasing between tropical and North Atlantic climate (assuming the methane has a tropical origin), the non-zero methane emissions of boreal sources across the Bølling transition complicate extrapolating the phasing between ice core gases to the phasing between regions. Using the changes in source distribution implied by the methane inter-polar difference reported in ref. 18, we estimate that boreal sources alone could contribute about 22% of the total methane increase across the Bølling transition, or approximately 32 parts per billion (ppb) of the 144 ppb total increase (Supplementary Table 2). If these boreal sources turned on first, we find that tropical sources could lag methane concentrations by, at most, 40 years, unless there was a transient pulse of methane from entirely boreal sources (Fig. 1), in which case, we find a maximum tropical lag of 67 years (Supplementary Text 6).

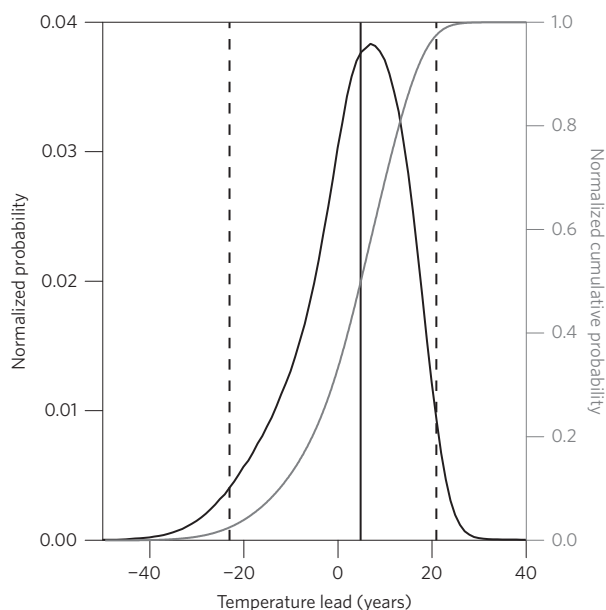


**Figure 4 | Phase relationship between Greenland temperature and methane emissions at the Bølling transition.** The normalized pooled (black) and cumulative pooled (grey) histograms of the phase lag (modelled surface temperature start time minus methane emission start time) at the Bølling transition for 25 surface temperature histories and 30 methane emissions scenarios. The vertical black line marks the median of the cumulative histogram; the dotted vertical lines show the 95% confidence interval. The most likely lead of methane emissions over temperature is  $4.5^{+21}_{-24}$  years.

We draw three important conclusions from these results. First, because no methane sources are known in the immediate vicinity of Greenland, synchronous changes in temperature and methane emissions reveal rapid transmission of the Bølling climate signal over large spatial scales regardless of the origin of methane. Second, such rapid transmission nullifies the use of all but the most precise phase analyses to shed light on the cause of this abrupt climate change. Third, inherent uncertainties (that is, small analytical errors, firn smoothing and firn heterogeneity) complicate the interpretation of even very high-resolution ice core data, preventing us from distinguishing between significantly different atmospheric histories, and illustrating that ice core gas records from low-accumulation sites or climate intervals cannot be interpreted at sub-decadal timescales.

Our uncertainty estimates indicate that methane sources could lead Greenland temperature by up to 24 years. If tropical climate shares this phasing, our results agree within error with those of ref. 25, which finds a  $10 \pm 5$  year lead of tropical regions over high-latitude sites using the phasing of  $[\text{Ca}^{2+}]$  and deuterium excess in the North Greenland Ice Core Project ice core. Alternatively, with a maximum methane source lag of 21 years, our findings contrast with previous estimates based on lower-resolution and lower-precision ice core gas data from the GISP2 ice core, which found a 20–80 year lag of tropical methane emissions behind  $\delta^{15}\text{N}$  at the Bølling transition<sup>11</sup> (Supplementary Text 7). A similar lag has been identified for D–O events during Marine Isotope Stage 3 (ref. 26), although we note that different mechanisms may be at play in different events.

We identify a range of possible explanations for our results. First, our data could be consistent with a North Atlantic driver of abrupt climate change, such as a recovery of the MOC, provided the change itself was rapid<sup>27</sup>, or that it initiated sensitive dynamic feedbacks such as sea ice retreat<sup>28</sup>. Suitably rapid teleconnections to

low latitudes include the link between Northern Hemisphere snow and sea ice extent on the position of the ITCZ, which models suggest could alter tropical climate in a matter of years<sup>5</sup>, or the effects of sea surface temperature patterns on the wind and stationary wave systems that modulate tropical precipitation<sup>29</sup>.

We also note that recent work has revised the timing of Meltwater Pulse 1a to be synchronous with the Bølling warming within dating uncertainties<sup>30</sup>, raising the possibility that the two events are causally related. Meltwater Pulse 1a has also been suggested to contain a significant contribution from Antarctic meltwater<sup>30,31</sup>. In addition to reinvigorating the MOC, freshwater input to the Southern Ocean could cause rapid cooling and the expansion of Southern Hemisphere sea ice that could conceivably displace the ITCZ north from its southerly position during Heinrich Stadial 1 (ref. 5), restarting Asian methane sources<sup>32</sup>.

Last, although tropical hypotheses<sup>33</sup> have fallen out of favour in recent years<sup>34</sup>, the temporal relationships in our data do not preclude the possibility of an as-yet unknown low-latitude driver of climate change. In any case, this study constrains possible mechanisms to those that can act abruptly across large spatial scales.

## Methods

$\text{CH}_4$  and  $\delta^{15}\text{N}$  were measured at high resolution across the Oldest Dryas–Bølling/Allerød transition in the NEEM ice core (Fig. 1). The core site is located at  $77.45^\circ\text{N}$  and  $51.06^\circ\text{W}$ , along the northwest Greenland ice divide and was drilled to a depth at bedrock of 2,540 m between 2008 and 2012 by the NEEM project members<sup>35</sup>. The ice and gas age chronologies for the core are presented in ref. 36.

$\text{CH}_4$  was measured at Oregon State University according to the methods described in ref. 37. Samples were taken from 94 depths, 40 of which were measured in duplicate, at an average depth resolution of 14 cm. The pooled standard deviation<sup>38</sup> is given by  $s_p = \sqrt{\sum (x_{i1} - x_{i2})^2 / 2k}$ , where  $x_{i1}$  and  $x_{i2}$  are duplicate measurements at depth  $i$  for  $k$  depths, for these measurements is 4.3 ppb.

$\delta^{15}\text{N}-\text{N}_2$  was measured at the Scripps Institution of Oceanography according to the methods given in ref. 39. The pooled standard deviation is 0.003‰. One hundred and five depths were measured at 14 cm resolution, with 6 analysed in replicate. The entire 55 cm interval between 1,505.325 and 1,505.875 m containing the  $\delta^{15}\text{N}$  reversal shown in Fig. 2 was remeasured in 5 cm samples on a parallel piece of ice.

Received 11 November 2013; accepted 28 March 2014;  
published online 4 May 2014

## References

- Dansgaard, W. *et al.* Evidence for general instability of past climate from a 250-kyr ice core record. *Nature* **364**, 218–220 (1993).
- Peterson, L. C., Haug, G. H., Hughen, K. A. & Röhl, U. Rapid changes in the hydrologic cycle of the tropical Atlantic during the last glacial. *Science* **290**, 1947–1951 (2000).
- Brook, E. J., Harder, S., Severinghaus, J., Steig, E. J. & Sucher, C. M. On the origin and timing of rapid changes in atmospheric methane during the last glacial period. *Glob. Biogeochem. Cycle* **14**, 559–572 (2000).
- Broecker, W. S., Peteet, D. M. & Rind, D. Does the ocean–atmosphere system have more than one stable mode of operation? *Nature* **315**, 21–26 (1985).
- Chiang, J. & Bitz, C. Influence of high latitude ice cover on the marine Intertropical Convergence Zone. *Clim. Dynam.* **25**, 477–496 (2005).
- Wang, X. *et al.* Millennial-scale precipitation changes in southern Brazil over the past 90,000 years. *Geophys. Res. Lett.* **34**, L23701 (2007).
- McManus, J., Francois, R., Gherardi, J., Keigwin, L. & Brown-Leger, S. Collapse and rapid resumption of Atlantic meridional circulation linked to deglacial climate changes. *Nature* **428**, 834–837 (2004).
- Barker, S. *et al.* Interhemispheric Atlantic seesaw response during the last deglaciation. *Nature* **457**, 1097–1102 (2009).
- Kageyama, M., Paul, A., Roche, D. M. & Van Meerbeek, C. J. Modelling glacial climatic millennial-scale variability related to changes in the Atlantic meridional overturning circulation: A review. *Quat. Sci. Rev.* **29**, 2931–2956 (2010).
- Seager, R. & Battisti, D. S. *Global Circulation of the Atmosphere* 331–371 (Princeton Univ. Press, 2007).
- Severinghaus, J. & Brook, E. Abrupt climate change at the end of the last glacial period inferred from trapped air in polar ice. *Science* **286**, 930–934 (1999).



12. Severinghaus, J., Sowers, T., Brook, E., Alley, R. & Bender, M. Timing of abrupt climate change at the end of the Younger Dryas interval from thermally fractionated gases in polar ice. *Nature* **391**, 141–146 (1998).
13. Chappellaz, J. A., Fung, I. Y. & Thompson, A. M. The atmospheric CH<sub>4</sub> increase since the Last Glacial Maximum. (1). Source estimates. *Tellus B* **45**, 228–241 (1993).
14. Bergamaschi, P. *et al.* Inverse modeling of global and regional CH<sub>4</sub> emissions using SCIAMACHY satellite retrievals. *J. Geophys. Res.* **114**, D22301 (2009).
15. Wang, Y. J. *et al.* A high-resolution absolute-dated late Pleistocene monsoon record from Hulu Cave, China. *Science* **294**, 2345–2348 (2001).
16. Chappellaz, J. *et al.* Changes in the atmospheric CH<sub>4</sub> gradient between Greenland and Antarctica during the Holocene. *J. Geophys. Res. Atmos.* **102**, 15987–15997 (1997).
17. Dällenbach, A. *et al.* Changes in the atmospheric CH<sub>4</sub> gradient between Greenland and Antarctica during the Last Glacial and the transition to the Holocene. *Geophys. Res. Lett.* **27**, 1005–1008 (2000).
18. Baumgartner, M. *et al.* High-resolution inter-polar difference of atmospheric methane around the Last Glacial Maximum. *Biogeosciences* **9**, 3961–3977 (2012).
19. Tans, P. P. A note on isotopic ratios and the global atmospheric methane budget. *Glob. Biogeochem. Cycles* **11**, 77–81 (1997).
20. Matsunaga, N., Hori, M. & Nagashima, A. Diffusion coefficients of global warming gases into air and its component gases. *High Temp.-High Press.* **30**, 77–83 (1998).
21. Buizert, C. *et al.* Gas transport in firn: multiple-tracer characterisation and model intercomparison for NEEM, northern Greenland. *Atmos. Chem. Phys.* **12**, 4259–4277 (2012).
22. Koehler, P., Knorr, G., Buiron, D., Lourantou, A. & Chappellaz, J. Abrupt rise in atmospheric CO<sub>2</sub> at the onset of the Bolling/Allerød: *In-situ* ice core data versus true atmospheric signals. *Clim. Past* **7**, 473–486 (2011).
23. Grachev, A. & Severinghaus, J. Determining the thermal diffusion factor for Ar-40/Ar-36 in air to aid paleoreconstruction of abrupt climate change. *J. Phys. Chem. A* **107**, 4636–4642 (2003).
24. Guillevic, M. *et al.* Spatial gradients of temperature, accumulation and δ<sup>18</sup>O-ice in Greenland over a series of Dansgaard–Oeschger events. *Clim. Past* **9**, 1029–1051 (2013).
25. Steffensen, J. P. *et al.* High-resolution Greenland ice core data show abrupt climate change happens in few years. *Science* **321**, 680–684 (2008).
26. Huber, C. *et al.* Isotope calibrated Greenland temperature record over Marine Isotope Stage 3 and its relation to CH<sub>4</sub>. *Earth Planet. Sci. Lett.* **243**, 504–519 (2006).
27. Vellinga, M. & Wood, R. A. Global climatic impacts of a collapse of the Atlantic thermohaline circulation. *Climatic Change* **54**, 251–267 (2002).
28. Li, C., Battisti, D. S., Schrag, D. P. & Tziperman, E. Abrupt climate shifts in Greenland due to displacements of the sea ice edge. *Geophys. Res. Lett.* **32**, L19702 (2005).
29. Hostetler, S. W., Clark, P. U., Bartlein, P. J., Mix, A. C. & Pisias, N. J. Atmospheric transmission of North Atlantic Heinrich events. *J. Geophys. Res. Atmos.* **104**, 3947–3952 (1999).
30. Deschamps, P. *et al.* Ice-sheet collapse and sea-level rise at the Bolling warming 14,600 years ago. *Nature* **483**, 559–564 (2012).
31. Clark, P. U., Mitrovica, J. X., Milne, G. A. & Tamisiea, M. E. Sea-level fingerprinting as a direct test for the source of global Meltwater Pulse IA. *Science* **295**, 2438–2441 (2002).
32. Weaver, A. J., Saenko, O. A., Clark, P. U. & Mitrovica, J. X. Meltwater pulse 1A from Antarctica as a trigger of the Bolling–Allerød warm interval. *Science* **299**, 1709–1713 (2003).
33. Clement, A. C. & Peterson, L. C. Mechanisms of abrupt climate change of the last glacial period. *Rev. Geophys.* **46**, RG4002 (2008).
34. Chiang, J. C. H. & Friedman, A. R. Extratropical cooling, interhemispheric thermal gradients, and tropical climate change. *Ann. Rev. Earth Planet. Sci.* **40**, 383–412 (2012).
35. Members, N community. Eemian interglacial reconstructed from a Greenland folded ice core. *Nature* **493**, 489–494 (2013).
36. Rasmussen, S. O. *et al.* A first chronology for the North Greenland Eemian Ice Drilling (NEEM) ice core. *Clim. Past* **9**, 2713–2730 (2013).
37. Mitchell, L. E., Brook, E. J., Sowers, T., McConnell, J. R. & Taylor, K. Multidecadal variability of atmospheric methane, 1000–1800 CE. *J. Geophys. Res. Biogeosci.* **116**, G02007 (2011).
38. Nič, M., Jirát, J., Košata, B., Jenkins, A. & McNaught, A. (eds) *IUPAC Compendium of Chemical Terminology* (IUPAC, 2006) <http://goldbook.iupac.org/P04758.html>
39. Petrenko, V. V., Severinghaus, J. P., Brook, E. J., Reeh, N. & Schaefer, H. Gas records from the West Greenland ice margin covering the Last Glacial Termination: A horizontal ice core. *Quat. Sci. Rev.* **25**, 865–875 (2006).

### Acknowledgements

We wish to express our great appreciation for the efforts and collaboration of the NEEM ice core community. NEEM is directed and organized by the Centre for Ice and Climate at the Niels Bohr Institute and US NSF, Office of Polar Programs. It is supported by funding agencies and institutions in Belgium (FNRS-CFB and FWO), Canada (NRCan/GSC), China (CAS), Denmark (FIST), France (IPEV, CNRS/INSU, CEA and ANR), Germany (AWI), Iceland (Rannls), Japan (NIPR), Korea (KOPRI), the Netherlands (NWO/ALW), Sweden (VR), Switzerland (SNF), the United Kingdom (NERC) and the USA (US NSF, Office of Polar Programs). We also acknowledge support from US NSF Grants OPP0806414 (to E.J.B.), OPP0806377 (to J.P.S.), ANT0806377 (to E.J.B.) and an NSF Graduate Research Fellowship (to J.L.R.). We thank R. Beaudette for making the δ<sup>15</sup>N measurements at the Scripps Institution of Oceanography.

### Author contributions

J.L.R. analysed the NEEM gas data, developed the firn air model, carried out the phase analysis and wrote the manuscript. E.J.B., J.P.S. and T.B. developed the initial hypothesis, assisted with analysis and oversaw measurement campaigns. L.E.M., J.E.L. and J.S.E. measured the methane samples. V.G. provided water isotope data and insight into chronology development. All authors provided input for the manuscript.

### Additional information

Supplementary information is available in the [online version of the paper](#). Reprints and permissions information is available online at [www.nature.com/reprints](http://www.nature.com/reprints). Correspondence and requests for materials should be addressed to E.J.B.

### Competing financial interests

The authors declare no competing financial interests.